THE NEW SATURNE INJECTOR

STATUS REPORT ON THE 20 MeV LINAC

JM. Lefèbvre - M. Promé - C. E. N. Saclay (France)

The proton linear accelerator, new injector for the Saturne synchrotron (I), is an Alvarez structure, with a final energy of 20 to 20.6 MeV, and an input energy of 750 keV. The current requirements are 20 mA for a 625 µs impulsion time, R.F. pulse being 1 ms long. Maximum repetition rate is 1 Hz.

The linac is now completely assembled ; all main equipments are either ready to be used or being checked. In this paper, details will be given on some particular aspects of this linear accelerator : technology, accelerating cavity, R. F. power supply and expected beam behaviour.

1 - Technology

1.1. - Resonant cavity °

The resonator is a cylinder 1 m in diameter and 10.5 m long. The cavity is made of four sections assembled by flanges (fig. 1). These sections are made of O.F.H.C. copper clad steel (5 mm Cu and 20 mm steel) sheets rolled and welded first on steel then on copper : the electrical conductivity of the copper weld has been found to be 80 % of O.F.H.C. copper.

The necessity of copper to copper contact at the junction planes of sections imposed good tolerances on rolling, the maximum errors were + 0.8 mm and - 0.5 mm for the average diameter on a section and ± 0.3 mm on ends diameter ; the error on total length of 4 sections is 0.45 mm.

The alignment principle provides only very small adjustments of the longitudinal position of drift tubes (§ 1.3) therefore the tolerances on positions of drilled holes in sections for fitting drift tubes had to be ± 0.2 mm with respect to the input end of the linac.

The good quality of welding and surface condition of copper insured a Q value equal to 80 % of the theoretical value after rolling and complete machining.

° The linac accelerating structure has been constructed by "C.S.F." company.

1.2. - Drift tubes fabrication °

The 59 drift tubes have been fabricated from sound technologies from the point of view of vacuum technique (fig. 2) : high temperature melting brazing and electron bombardement welding.

Two leaks only have been detected, at the junction of bellow on supporting stem. Machining precision on drift tubes are ± 0.05 mm.

Diamant powder of decreasing size have been used for final polishing.

The supporting stem (fig. 3) is made of two concentric tubes. The stainless steel inner tube insures mechanical strength and vacuum tightness while the copper tube is for R.F. currents conduction.

The stem is fitted to the drift tube by an argon arc welding on steel, then electrolytic copper is deposited on the outer copper tube for insuring the continuity. Inside drift tube bodies are enclosed D.C. fed quadrupoles.

In first quadrupoles magnetic gradients are of the order of 50 $T.m^{-1}$ which corresponds to a current of 500 A, cooling is therefore a difficult problem, water is let into the pipes of the coils at a pressure of 20 bars. A cooling circuit is also brazed inside the drift tube body for temperature stabilisation.

1.3. - Drift tubes alignment

On the top part of the stem is brazed a copper bellow (fig. 4) which gives provision for rotation in both xoz and yoz planes plus translation in z direction (fig. 5). These motions are controlled by adjusting screws (fig. 6).

Alignment has been made from a telescope centered on a reference axis and optical targets fitted in the drift tube bore.

Alignment precision have been ± 0.1 mm for x and z positions, and ± 0.3 mm for y direction.

An optical target holder fitting on the top end of the stem allows for alignment control of the drift tubes without breaking vacuum (fig. 7).

1.4. - Vacuum system

The roughing unit consists of a mechanical pump, a roots blower and a 2 000 l/s true pumping speed turbomolecular pump. This system enables reaching a pressure of 10^{-5} torr after 8 hours of pumping. A hot water circulation in an envelope around the cavity can raise the cavity body temperature up to 70° C within 5 hours in order to improve outgassing.

Secondary pumping is from 4 ion pumps with a 3 000 l/s true total pumping speed. A 10^{-6} torr pressure is obtained after 75 hours of pumping.

2 - Electrical properties of the accelerating cavity

The dispersion on section diameters have been compensated by tuning bars fitted to the bottom of each section. These bars dimensions have been estimated from resonant frequency measurements on each of four sections without drift tubes.

Nineteen ball tuners spread along the accelerating structure allow fine adjusting of the field on the axis (the linac has to be operated with a constant mean field) ; ball tuners diameter is 100 mm, supporting stems diameter is 10 mm. Ball tuners produce a 600 kHz frequency shift when moved all together on their 200 mm maximum range. First measurements showed that the field was completely perturbated for certain positions of the ball tuners ; for these positions, the Q factor was surprisingly low ; a correct explanation for this phenomenon involves a parasitic mode which looks like a stem-mode. The capacitance of the ball with respect to the cavity wall together with the inductance of the stem supporting the ball behave like a resonator ; troubles arise when the resonance frequency of this resonator is close to the Alvarez frequency ; a frequency sweeping of the cavity

° The linac accelerating structure has been constructed by "C.S.F." company.

showed that for certain positions of ball tuners this low Q stem-mode was superimposed on the Alvarez mode, which disappeared. We got rid of this difficulty by insulating the ball tuners from their supporting stems ; then, the stem-mode resonance frequency was much higher and no longer produced undesirable effects.

Electrical field on the axis has been measured by the classical perturbation method. A 7 mm diameter copper bead was used ; maximum frequency shift was 300 Hz.

A field recording along the 10.5 m long structure required 30 minutes. Instead of evaluating the mean field in the cells, which is obtained by integration of the actual field, the mid-gap field values were compared to the ideal mid-gap values supplied by the IDDA program (II).

Figure 8 shows the first recording of the electrical field on the axis ; all ball tuners were at the same radial position from the axis. Figure 9 shows the field after modification of the sizes of the tuning bars ; again ball tuners were at the same radius. Figure 10 shows the field after setting ball tuners in adequat positions ; these positions have been derived by the J.L. Walters' method (III).

Three ball tuners among 19 are included in a servo loop which keeps the cavity resonance frequency constant ; (temperature control of the cavity is within $\pm$ 0.5° C) ; when moved together the three ball tuners needed displacement for compensating the effect of this temperature drift is 20 mm ; it has been checked that such a displacement has no significant effect on the field on the axis.

The Q coefficient is slightly dependent upon the ball tuners positions ; for the operating positions Q = 75.000. The theoretical value being 99.000. The theoretical value of the shunt impedance is 79 MΩ/m, the actual value may be estimated to be 60 MΩ/m. 1.3 MW are then required to set the field at its nominal value, without beam loading compensation.

Mode spacing has been measured 330 kHz have been found between E_{011} and E_{010} ; 1.45 MHz between E_{012} and E_{010}.

3 - R. F. Power supply °

A schematic of the R.F. power supply is shown on figure 11 ; power figures are maximum available power ; in particular 2 MW fed into the accelerating cavity should be enough to handle a 35 mA, 650 µs long beam.

Amplifiers stages equiped with triodes TBL 6/20 and TH 470 are grounded grid ; their plate voltage is permanently applied ; without R.F. signal the tubes are cut off by adequat bias applied on their cathodes.

The final stage is equiped with a grounded grid TH 515 triode ; it is plate modulated by a TH 500 triode acting as a hard tube.

TH 470 and TH 515 stages are equiped with a crowbar system ; the crowbar tubes are General Electric ZG 7 248 ignitrons.

4 - Expected beam behaviour

4.1. - Predicted effect of R.F. level

This linac has been devised so that the stable phase angle is varied continuously from - 45° at low energy up to - 25° at high energy. The R.F. threshold below which particles are no longer accelerated is not as well defined as for a constant stable phase angle linac ; R.F. level may be such that particles are accelerated in the first part of the linac only, then drift along the remaining part of the linac, experiencing a null mean accelerating effect, and appear at the exit of the linac with an energy below 20 MeV ; if this energy is sufficiently close to 20 MeV, radial losses may be small.

° The linac R.F. power supply has been constructed by "C.F.T.H." company.

Computations have been carried out with the general beam dynamics program which has been used to determine the linac ; mean electrical field which was taken into account in these computations was kept constant along the linac, with a value E which entered as a datum for the program, while E_n was the nominal E value. The injected beam was chosen with emittances equal to the actual emittances obtained with the preinjector ; moreover the emittances were matched to fill the central area of the linac admittances. The double buncher was in operation.

Figure 12 shows the variation of the output energy with respect to the E/E_n ratio : the output energy is practically constant above $E/E_n = 0.9$.

Figure 13 shows the total number of outcoming particles which is also practically constant above $E/E_n = 0.9$. ; this figure shows also the number of outcoming bunched particles ; this number remains constant only above $E/E_n = 0.95$.

4.2. - Matching of the 750 keV beam emittance to the linac admittance

Beam emittance areas at the linac input are substantially smaller than the linac admittance areas in X and Y, since :

ε_n = emittance area . $\beta\gamma$
$\simeq 2.5.10^{-6}$ m.rd (measured value) (IV)

$A_{n.50}$ = admittance area for 50 % . $\beta\gamma$
$\simeq$ 18 mm.m.rd

$A_{n.80}$ = admittance area for 80 % . $\beta\gamma$
$\simeq$ 9 mm.m.rd

Values 50 % and 80 % are referred to W, Φ capture efficiency with the double buncher in operation ; maximum capture efficiency, obtained for :

$X = X' = Y = Y'$

is 84 %.

A good matching requires : first, a good choice of ellipses excentricities, which can be met by adjusting quadrupole currents in the beam transport system between the preinjector and the linac ; second, right slopes of these ellipses on their axis.

Some computations have been undertaken to see the influence of the linac first quadrupole (located in the first drift tube) on the admittances slopes ; figures 14 to 17 summarize the results of these computations. B'_n being the nominal gradient, derived by continuity from the other linac quadrupole gradients, $B' = 0.8\ B'_n$ and $B' = 0.65\ B'_n$ have been tried ; the influence in the X direction is rather small, while one obtain a significant change in the Y slope without changing too much the total area ; thus, the first quadrupole may be conveniently used for emittance matching.

REFERENCES

I J. Faure et al
"A new injector for the Saturne synchrotron" - Proceedings of the International Conference on High Energy Accelerators (Frascati, 1965).

II M. Promé
"Design of a 20 MeV proton linear accelerator, new injector for Saturne" - Proceedings of the 1966 linear accelerator conference - L.A. 3609

III J.L. Walters
"Flattening procedure for empty cylindrical cavities" - B.N.L. internal report - J.L.W. 1

J.L. Walters
"The ball tuner change tables"
B.N.L. internal report - J.L.W. 2

IV J. Faure
"The new Saturne injector - Status report on the 750 keV preinjector"
published in these Proceedings p.240.

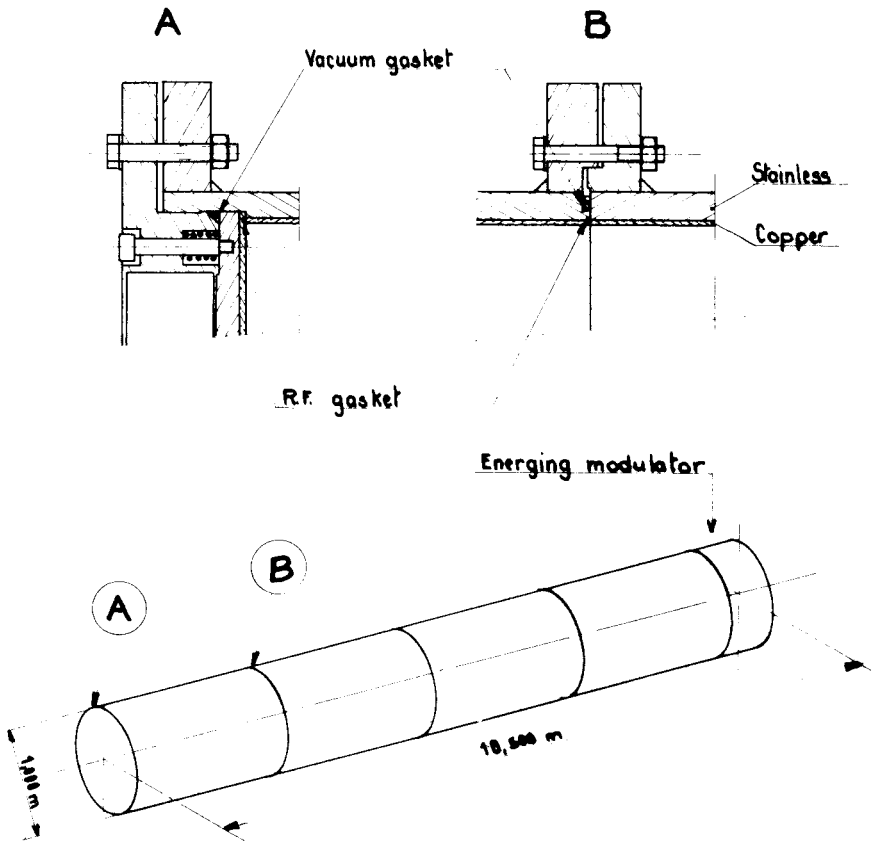

Figure 1) Flange details

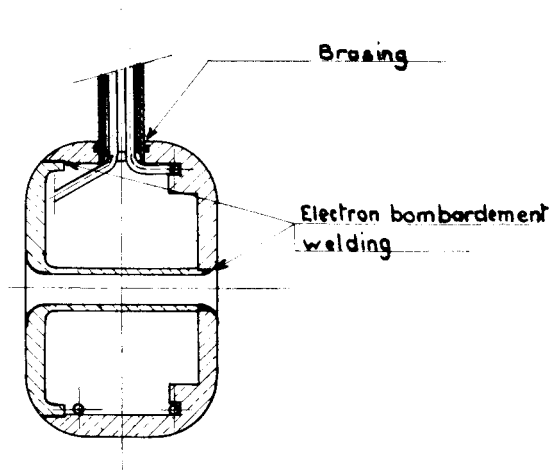

Figure 2) Drift tube detail

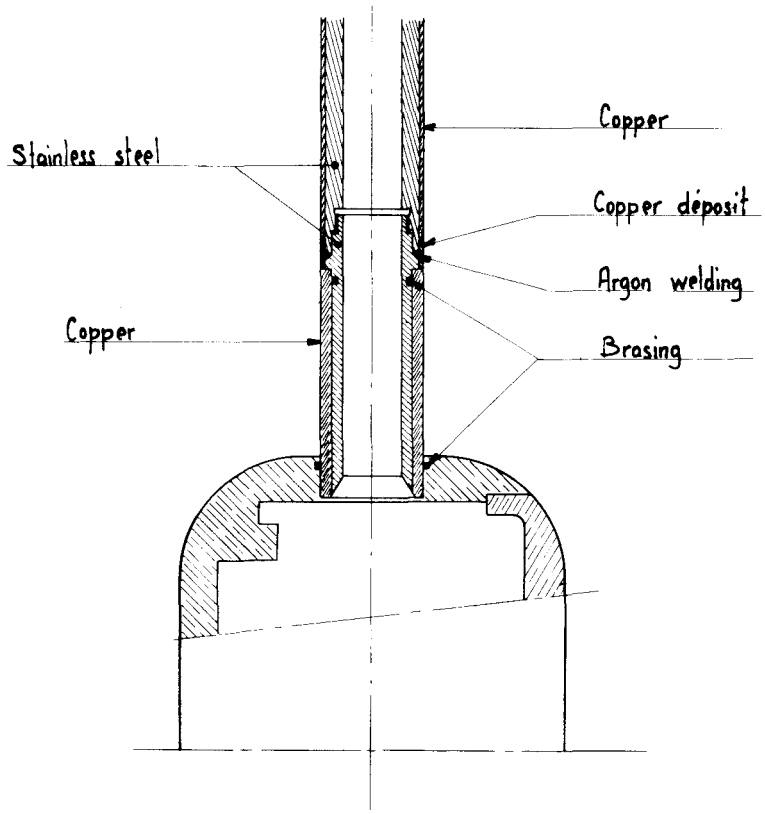

Figure 3) Drift tube supporting stem detail

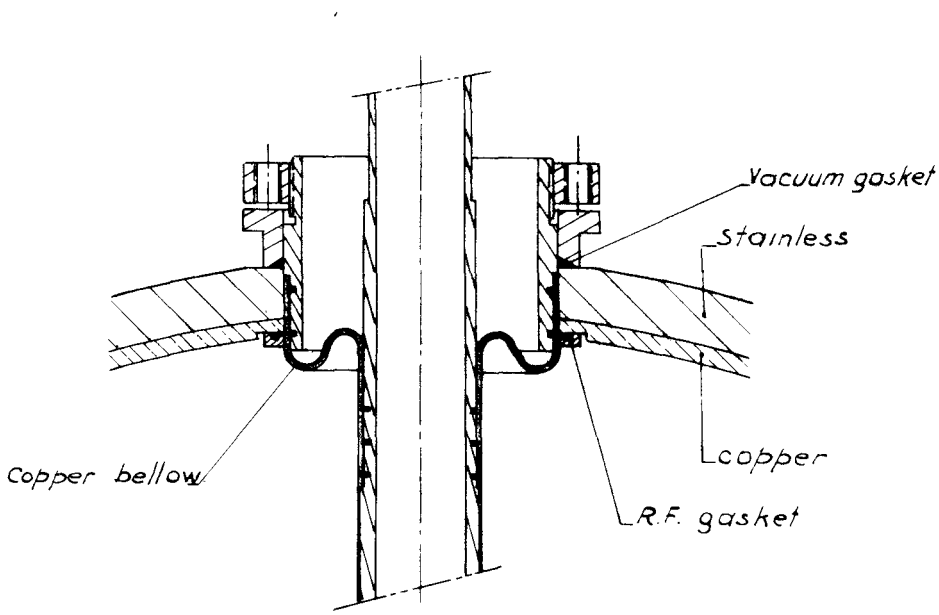

Figure 4) Top part of stem with provision for rotation and translation

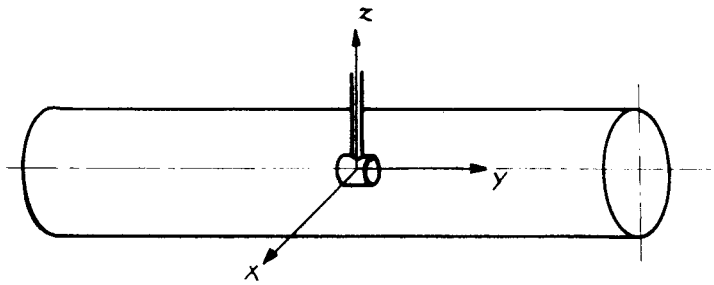

Figure 5) Drift tubes can be rotated in both xoz and yoz planes and translated in the z direction

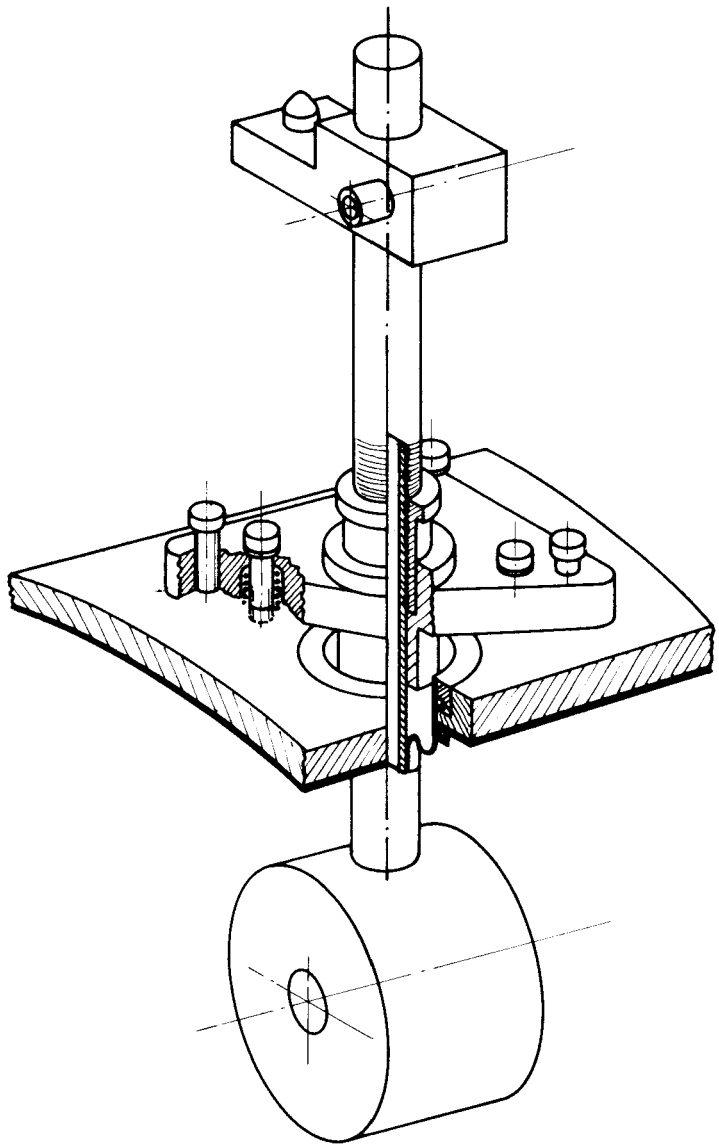

Figure 6) Adjusting screws for controling motion of a drift tube

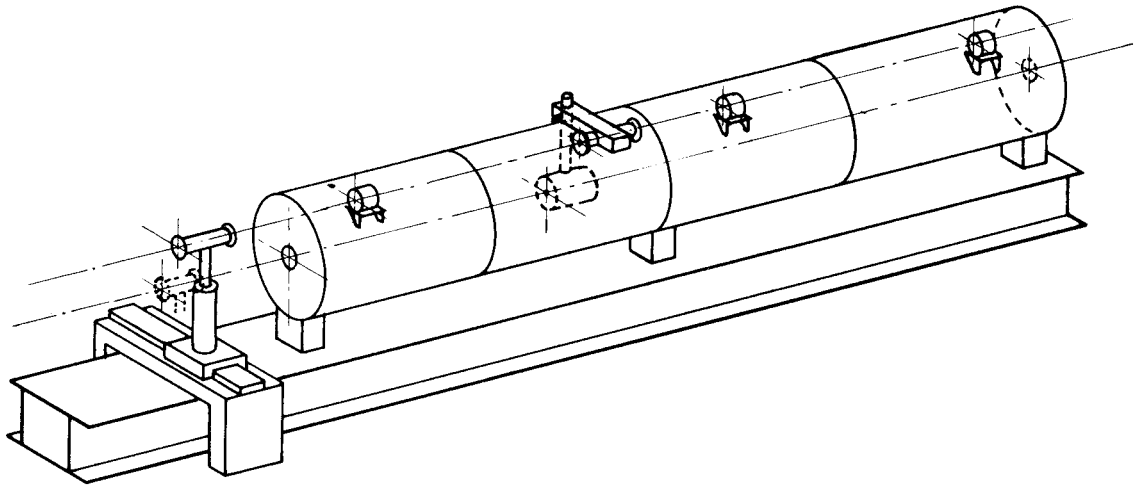

Figure 7) Optical alignment system

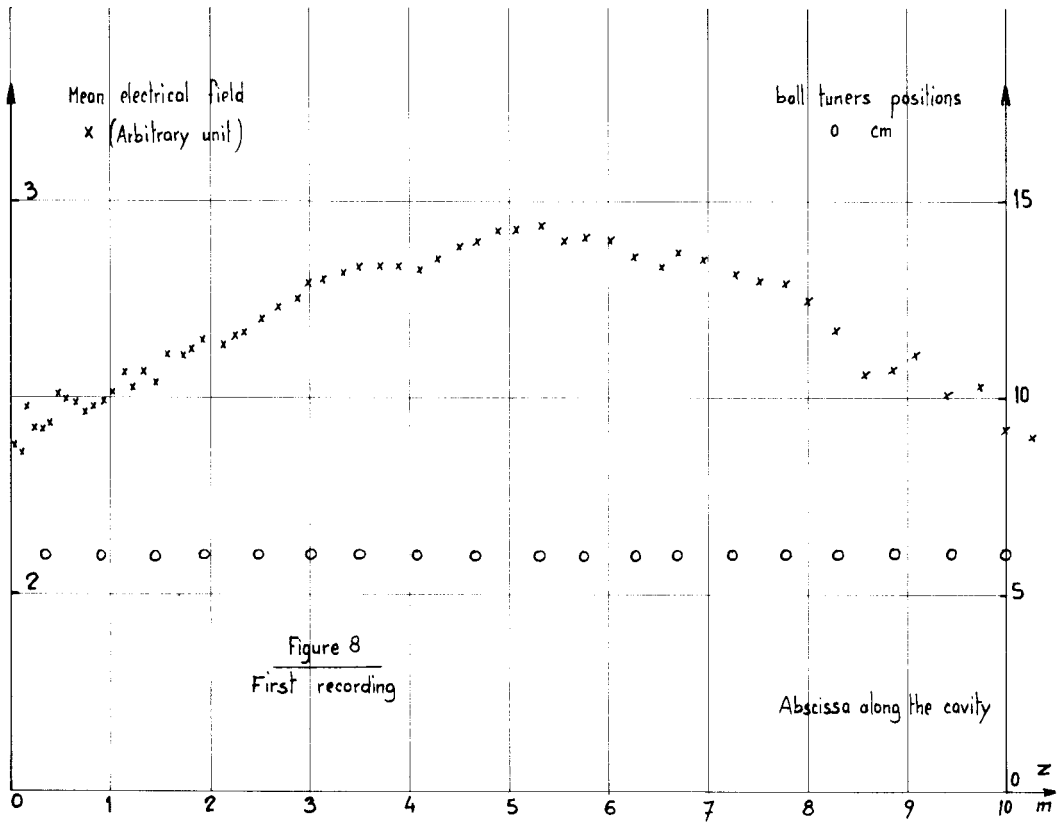

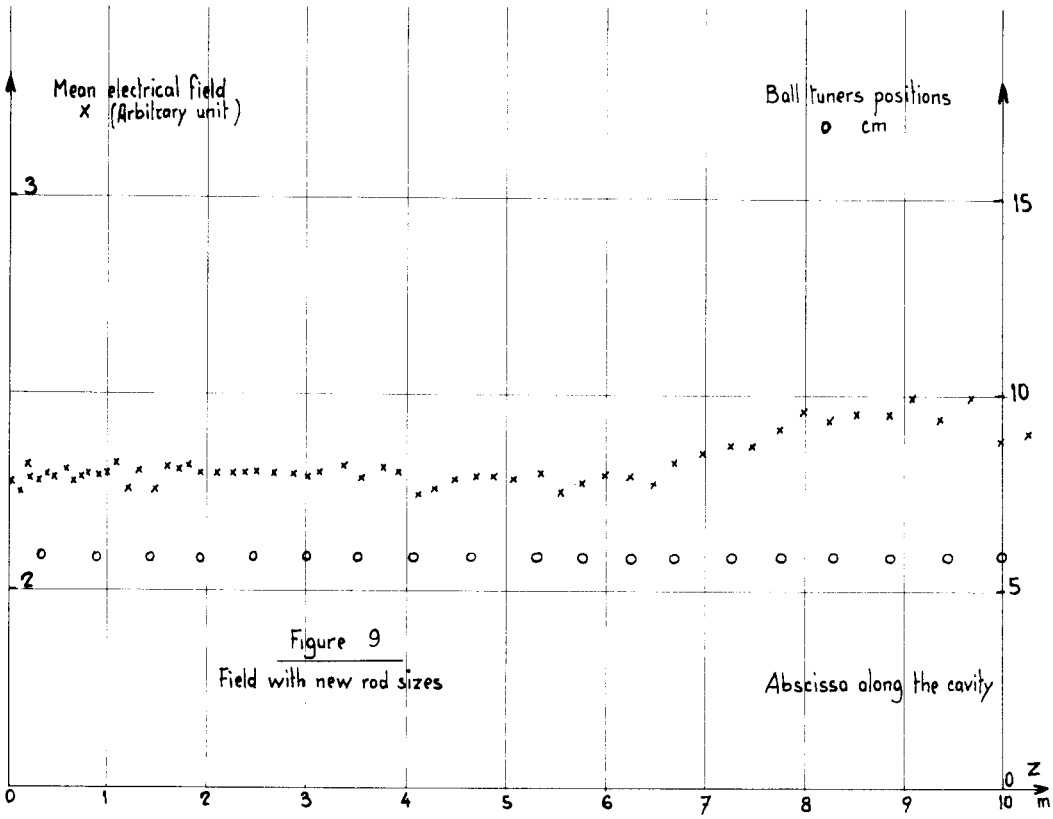

Figure 9
Field with new rod sizes

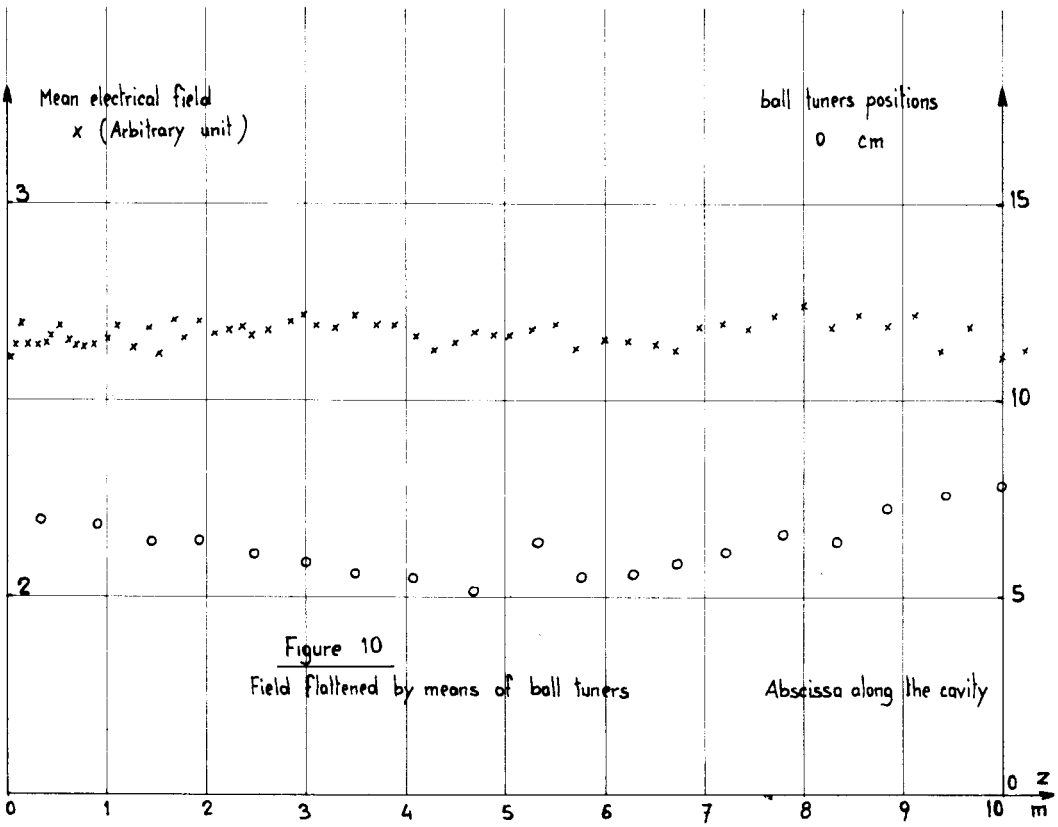

Figure 10
Field flattened by means of ball tuners

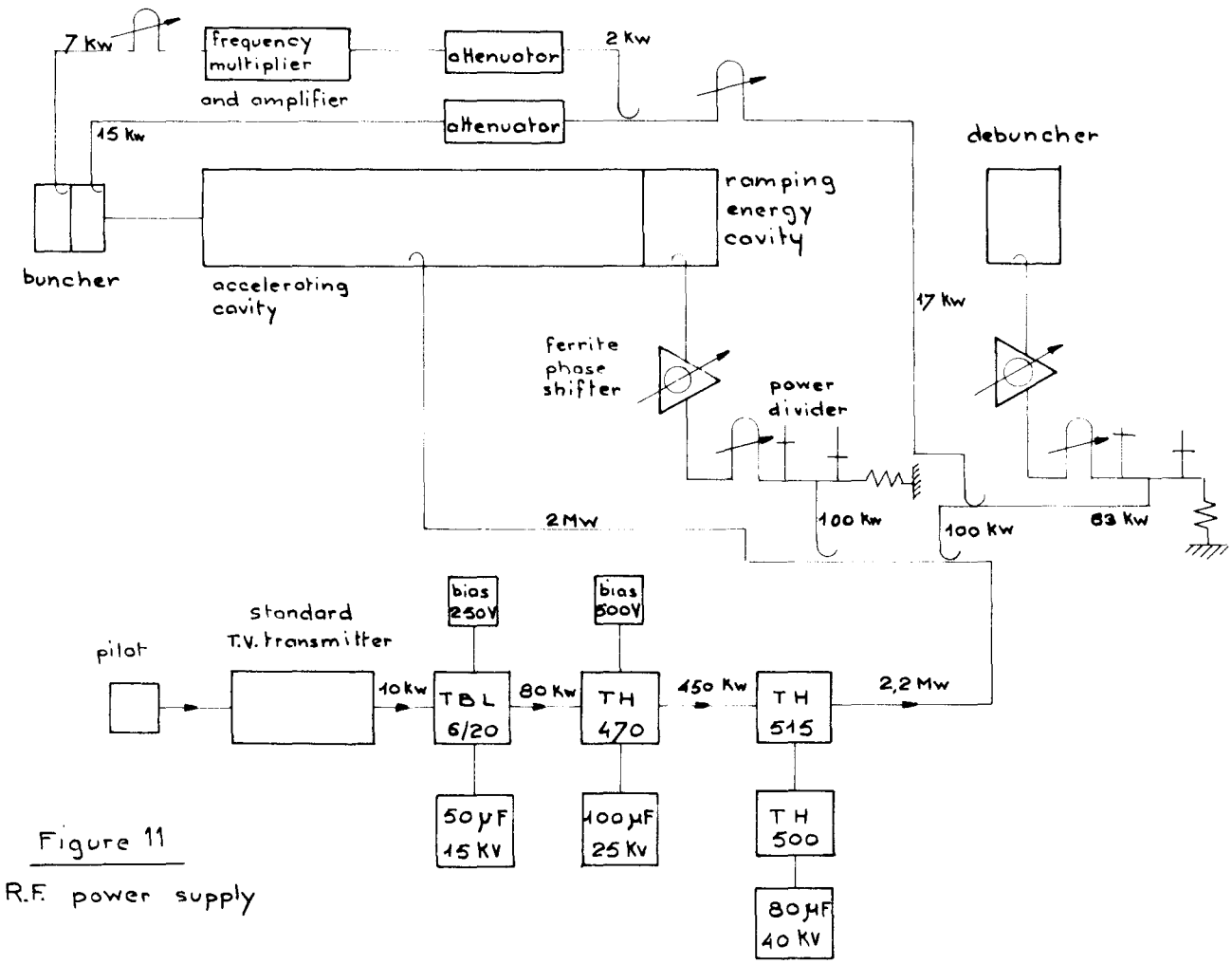

Figure 11

R.F. power supply

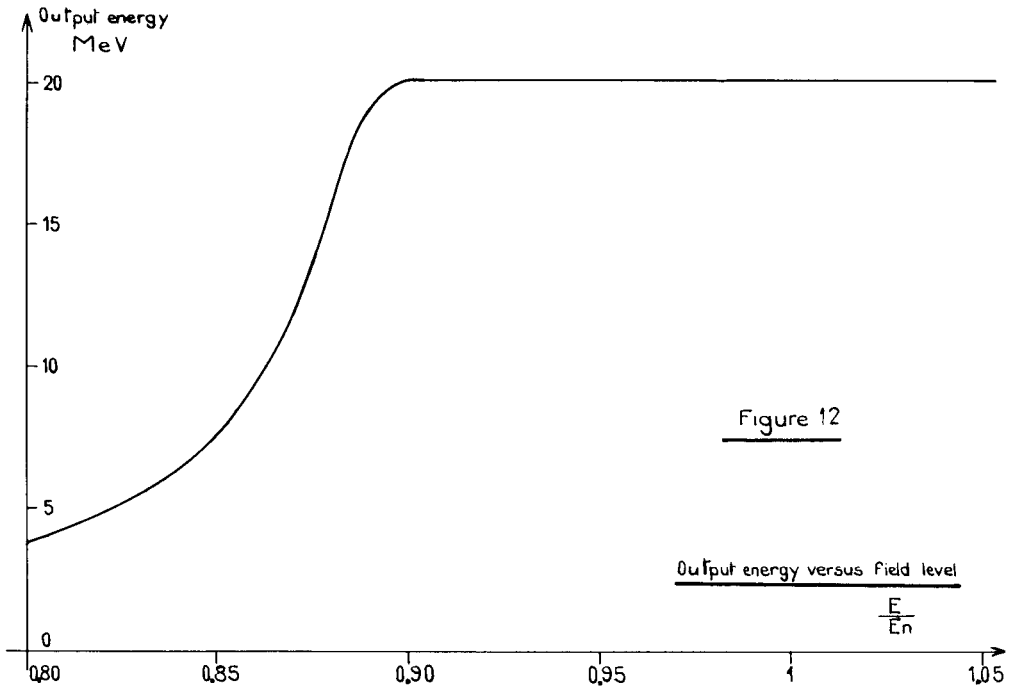

Figure 12

Output energy versus field level

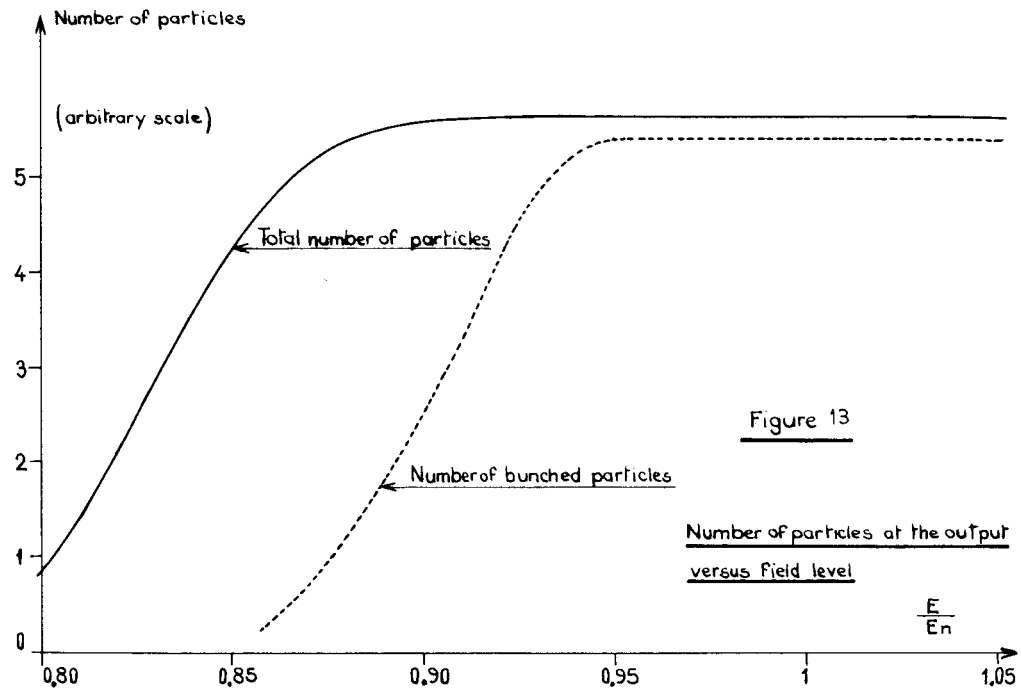

Figure 13

Number of particles at the output versus field level

FIGURE 14

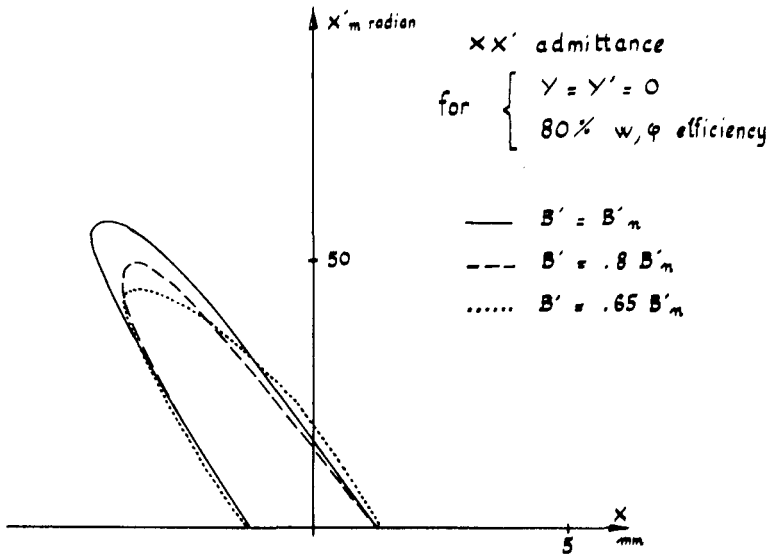

FIGURE 15

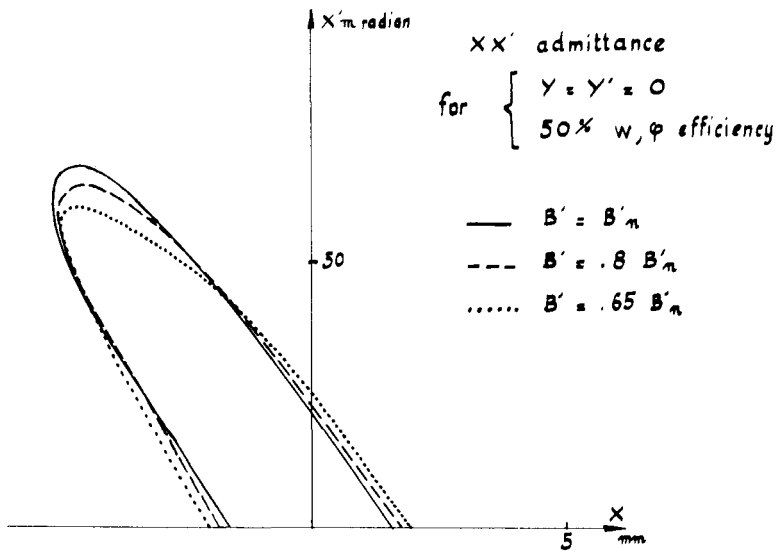

FIGURE 16

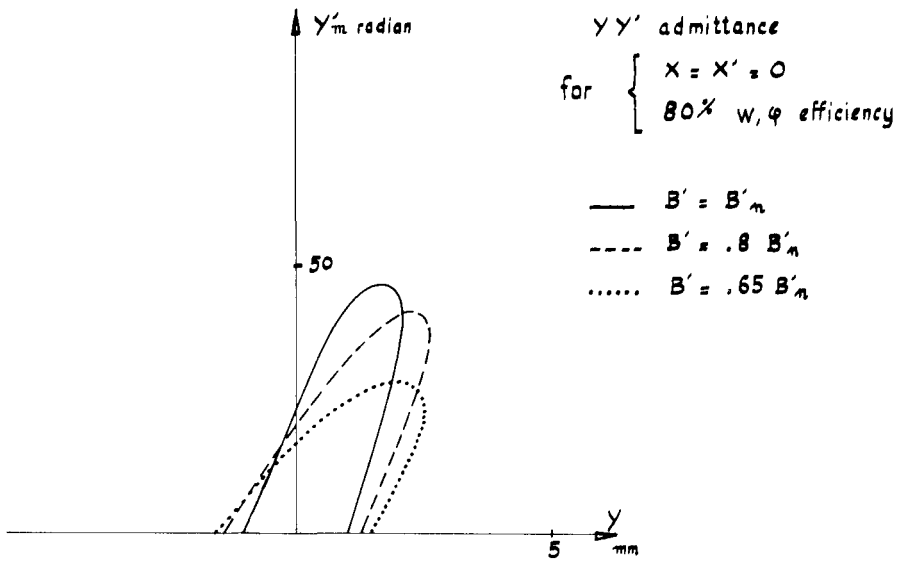

FIGURE 17